



Expanding Fluidized Zones: A Model of Speed-Invariant Lubricity in Biology

Angela A. Pitenis¹ · Alison C. Dunn^{2,3} · W. Gregory Sawyer⁴

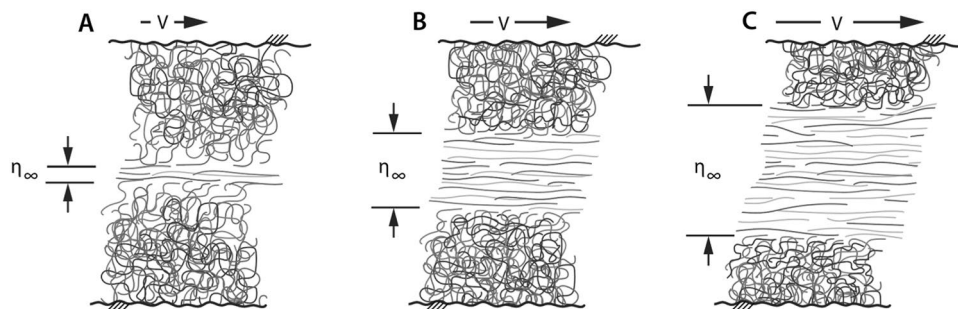
Received: 25 February 2023 / Accepted: 25 April 2023 / Published online: 31 May 2023
© The Author(s), under exclusive licence to Springer Science+Business Media, LLC, part of Springer Nature 2023

Abstract

A simple model for speed-invariant shear stress in biological aqueous lubrication has been developed based on previous observations of these fluid films and our foundational understanding of these complex fluids. The model revealed that the exponent of the shear-thinning behavior is not a critical parameter in speed invariance. Additionally, due to the localization of fluidization as a result of gradients in concentration through the aqueous gel network, the shear-thinning behavior results in a monotonic decline in viscosity to the high shear-rate viscosity plateau, η_{∞} . Finally, and perhaps somewhat surprising, was the finding that the optimal gradient was the weakest possible gradient. These findings are consistent with our understanding of aqueous lubrication across soft biological interfaces, which is sensitive to the macromolecular quality of the gel-spanning networks and the water content but not the sliding speed. The finding that this speed-invariant shear stress does not require a unique concentration profile reveals a built-in mechanism of biological resilience to maintain lubricity over a wide range of conditions.

Graphical Abstract

Gradients in concentration localize fluidization at the lowest concentration regime during sliding. This leads to an expanding shear zone with proportionally thicker fluidized zones for increasing values of sliding speed resulting in roughly equivalent shear rate and shear stress for all sliding speeds



Keywords Biotribology · Mucin Networks · Synovial Fluid · Lubrication · Aqueous Lubrication

✉ W. Gregory Sawyer
wgsawyer@ufl.edu

- ¹ Materials Department, University of California Santa Barbara, Santa Barbara, USA
- ² Department of Mechanical Science & Engineering, University of Illinois Urbana-Champaign, Urbana, IL, USA
- ³ Department of Biomedical & Translational Sciences, Carle Illinois College of Medicine, Urbana, IL, USA
- ⁴ Department of Mechanical and Aerospace Engineering, University of Florida, Gainesville, USA

As de Gennes wrote in his introduction to the 2007 edited book *Superlubricity*, soft systems are a ‘gold mine’ of opportunity for research in lubricity [1]. As Dowson often discussed, the lubricity of cartilaginous joints is likely the most studied and debated natural system, which maintains homeostasis and low shear stress across soft articular cartilage via a cacophony of potential mechanisms (e.g., soft elastohydrodynamic lubrication [2, 3], Gemini gel

lubrication [4–12], proteinaceous aqueous shear-thinning synovial fluid [13–15], and many others [16–21]). Although the importance of joint lubrication has long been recognized [22–24], the lubricity across epithelial interfaces via mucin networks (e.g., the tear film, human tissue interfaces, the digestive tract, and the reproductive tract) may represent the most abundant interfaces by both distribution and contact area [25, 26].

In human biology, the lubricity within interfaces of epithelia and cartilage is achieved by high water-content gel-spanning networks of hydrophilic biomacromolecules arranged into complex ensembles containing proteoglycans, mucins, glycosaminoglycans, hyaluronic acid, and many other components [27]. These fragile aqueous gels are formed through both entanglements and weak ‘flickering’ bonds that enable the gel to fracture, which limits the shear stress to the failure stress of the gel [27–29]. Once fractured, we propose that these macromolecules collectively create a strongly shear-thinning fluid that expands the shearing zone in response to sliding speed to maintain a constant shear stress. Central to this hypothesis is the need for gradients to provide an initiation and a graceful expansion yielding nearly constant shear stress independent of sliding speed.

Conventional hydrogels, in contrast to weak ‘flickering’ bonds of natural lubricants in the human body, are comprised of relatively strong, permanently crosslinked macromolecules with a characteristic conformational dimension, ξ ; the mesh size, ξ , is also approximately equal to the swollen size of the macromolecule in solution, $\xi \sim R_g$. Swollen hydrogels therefore exist right at the critical overlap concentration, c^* , where the spacing between macromolecules, L_D , the mesh size, ξ , and the radius of gyration, R_g , are all of the same order of magnitude: $\xi \sim R_g \sim L_D$ [9, 30, 31]. These gels are distinct from brushes, where $L_D < R_g$ and the macromolecules are squeezed together into the brush conformation. A major difference between conventional hydrogels

and the fragile gels spanning our biological interfaces is the strong irreversible crosslinks of hydrogels that prevent the graceful fracture and regelation ubiquitous in biology.

The classic engineering model of fluid lubrication is the Stribeck curve, which at low sliding speeds has a friction coefficient regime called *boundary lubrication* that then transitions to *mixed lubrication* with increasing sliding speed [32]. This transition from boundary lubrication to mixed lubrication has a rapidly decreasing friction coefficient with increasing sliding speed. A decreasing friction coefficient with increasing sliding speed is a type of instability that can manifest as stick–slip [33], such as the ‘squeaking hips’ problem that emerged in total hip replacements [34] or the pleural and pericardial friction rubs within the inflamed chest cavity [35, 36]; healthy biological lubrication appears to be absent of such instabilities. The ocular surface has the greatest innervation density of any tissue in the human body [37], and continuous fine movements are required during waking activities; such an interface would be expected to be exquisitely sensitive to instabilities. Approximately once every 6 s, the eye undergoes a rapid blink where speeds between the eyelid and the cornea reach speeds on the order of 100 mm/s [38]. Most of this happens with no perceived difference in shear stress. Interestingly, and as another example, early pendulum testing of animal joints repeatedly suggested a steady and low values of friction coefficient even through motion reversals [22].

A simple hypothesis for the apparent speed-independence of shear stress in these biological gel-spanning networks that is consistent with our understanding of these complex fluids has been elusive. A few of the ubiquitous findings of these fragile aqueous gel networks include: (1) these fluids are shear thinning, but not with a shear exponent of exactly -1 [39], (2) the high shear-rate viscosity approaches that of water [40], (3) there are gradients in macromolecular concentration through the gel [27, 41, 42], and (4) the yield

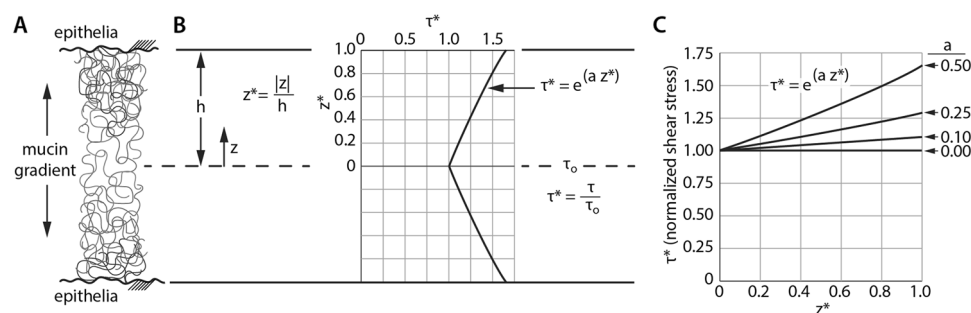


Fig. 1 Schema of model development. **A** Cross-section of a gel-spanning mucin network with decreasing mucin concentration toward the center. The dimensionless parameter, z^* , is positive in both directions from the center and is normalized by the film half-

thickness, h . **B** A generic, normalized shear stress model across the tear film, τ^* plotted as a function of z^* based on an exponential function. **C** Plot of the normalized shear stress as a function of location through the film and the exponent constant, a

stress of the gels is proportional to the macromolecular concentration [27].

The initial hypothesis that we followed was that the gradients in macromolecular concentration were the key to the speed invariance, and the model developed below began by assuming an unknown exponential form of the yield stress as a function of position through the film (Fig. 1 and Eq. 1). The fluid film in this case is envisioned as a mucin gel-spanning network between two epithelia and will be discussed as such during model development although the model is equally envisioned to be broadly appropriate for biological lubrication, including joints.

As previously mentioned, the model begins from a generic assumption of an exponential form of the yield-stress that is minimum at the central location of the film, τ_o . The exponential function was chosen to be a simple function that allowed for the strength of the gradient to be easily controlled by a single parameter, a , the network yield-stress gradient exponent, and facilitates trivial integrals and derivatives. Note that in this model the position, z , is positive in both directions, and z^* is given by Eq. 2, where the gel film half-thickness is h . The variables are illustrated in Fig. 1.

$$\tau = \tau_o e^{az^*} \tag{1}$$

$$z^* = \frac{z}{h} \tag{2}$$

Based on extensive rheological characterization of high-water-content bio-macromolecular gels, it is essentially established that they all show strong shear thinning [43]. Shear thinning is important to this model, but it is the behavior of shear thinning that is important not the actual shear-thinning exponent, b (Fig. 2A). Although the apparent viscosity monotonically decreases with increasing shear

rate, the increasing shear rate with increasing sliding speed eventually causes the shear stress to exceed the local yield stress, which in turn causes local yielding at the interface and further expansion of the fluidized zone. Once the shear rates reach the threshold for the lower viscosity plateau, any further increases in sliding speed further increase the shear stress linearly; this eventually exceeds the yield stress at the peripheral interface, which again causes interfacial yielding and an increase in the fluidized zone thickness. Note that Fig. 2 illustrates an interesting finding in that the actual shear rate at which this shear-rate independence occurs is unimportant; what is important is that it exists! Once the gel yields, the fluidization monotonically drives to the minimum high shear-rate viscosity. Given the assumed Couette flow profile of the fluidized zone, the resulting fluid shear stress at any speed, V , is then simply given by Eq. 3.

$$\tau = \eta_\infty \frac{V}{2hz^*} \tag{3}$$

The model development continues by equating the yield stress at the border of a particular fluidized range of z^* to the fluid shear stress within the fluidized zone given by Eq. 3 giving the equality shown in Eq. 4.

$$\tau_o e^{az^*} = \eta_\infty \frac{V}{2hz^*} \tag{4}$$

Rearranging Eq. 4 into a dimensionless form gives reveals a new dimensionless group, which we assign as the dimensionless speed parameter, V^* , as shown in Eq. 5 and Eq. 6.

$$z^* e^{az^*} = \frac{\eta_\infty}{\tau_o} \frac{V}{2h} = V^* \tag{5}$$

$$z^* e^{az^*} = V^* \tag{6}$$

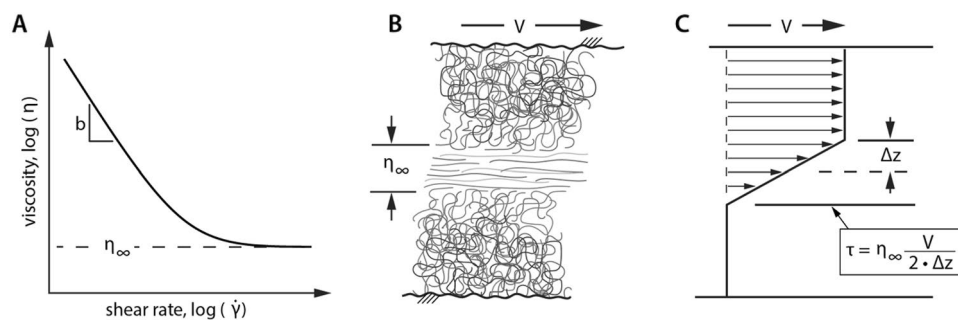


Fig. 2 **A** Biological fluids are well-known to exhibit shear-thinning behavior, which is indicated by a decreasing viscosity with increasing shear rate (log–log plot). At high shear rates (e.g., during an eyeblink) the fluid film viscosity may reach a lower plateau, defined as the infinite shear viscosity plateau, η_∞ . **B** In this model, a localization of fluidization in the lowest concentration zone causes the shear rate to

reach a level such that the fluidization shear stress equals the bounding gel yield stress, and due to the shear-thinning behavior, must go to the infinite shear viscosity plateau. **C** The fluidized region of the fluid film adapts in response to sliding speed, giving a fluidized zone with Couette flow behavior

Recognizing that Eq. 6 is actually the definition of the Lambert W function (represented by the symbol W) the closed form solution for the normalized half-thickness of the shear zone, z^* , is only controlled by two dimensionless parameters: the dimensionless speed, V^* , and the network yield stress gradient exponent, a .

$$z^* = \frac{W(aV^*)}{a} \tag{7}$$

Taking the solution for the normalized shear zone, z^* (Eq. 7), and substituting this back into the original expression for the yield stress gradient, Eq. 1, provides a closed form dimensionless expression for shear stress, Eq. 8, where the shear stress is normalized by the central shear stress at $z^*=0$ as shown in Eq. 9.

$$\tau^* = e^{W(aV^*)} \tag{8}$$

$$\tau^* = \frac{\tau}{\tau_o} \tag{9}$$

As shown in Fig. 3, the normalized shear stress is plotted as a function of the normalized sliding speed for various

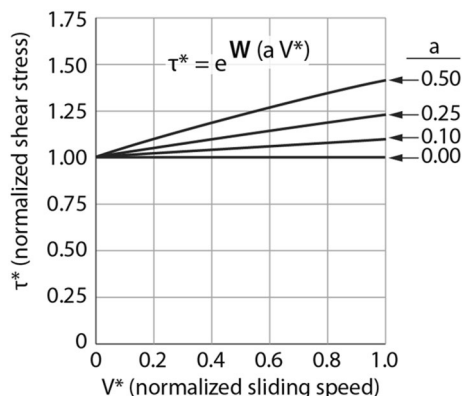
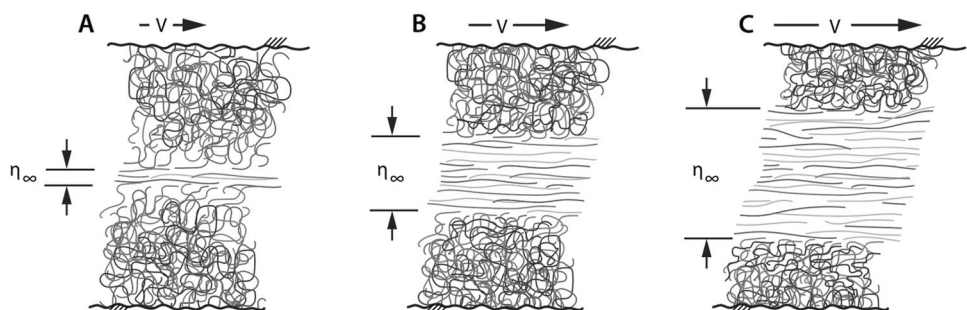


Fig. 3 Normalized shear stress, τ^* , is dependent upon the exponential product of the Lambert W function, normalized sliding speed, V^* , and the steepness of the mucin gradient, a . Decreasing the steepness of the mucin gradient (decreasing the thickness of the fluidized mucin region) gives rise to lower shear stress across the sliding interface

Fig. 4 Illustration of the expanding shear zone model for speed independent shear stress. A–C increasing values of sliding speed result in proportionally thicker fluidized zones of roughly equivalent shear rate and shear stress



exponents and revealed an initially surprising result that the optimal gradient in yield stress is the shallowest gradient that facilitates and controls yielding at the center of the film. We hypothesize that a gradient must exist in order to repeatedly control the location of fluidization, and the conceptual framework is thus that the thickness of the zone is continuously responding to the sliding speed and thereby maintaining a nearly constant shear stress independent of sliding speed (Fig. 4).

For completeness, the dimensional solution is provided in Eqs. 10 and 11.

$$\tau = \tau_o e^{W(aV^*)} \tag{10}$$

$$\tau = \tau_o e^{W\left(\frac{a\eta_\infty}{\tau_o} \frac{V}{2h}\right)} \tag{11}$$

As previously discussed, a simple hypothesis for the apparent speed-independence in biological aqueous lubrication consistent with our understanding of these complex fluids has been elusive. Following this model development, we recognized a number of parameters that we had initially assumed to be important were not represented in the solution. One of the first and potentially surprising findings is that the shear-thinning exponent is not a critical parameter; what *does* matter is the high shear-rate viscosity plateau, η_∞ . The other somewhat unexpected finding was that there really is no optimal gradient; the weakest gradient gives the most speed-invariant shear stress! This introduces a seemingly curious paradox in that a weak gradient has the least favorable conditions for initiating and maintaining fluidization in a particular zone; a weak gradient could have fluidized zones randomly initiate and arrest in different locations simultaneously. This apparent paradox is mitigated by the rheology of these weak flickering bonds on the terminal ends of the biomacromolecules. While the imposed shear stress causes a rapid rupture via the weakness of these flickering bonds, the comparatively long thixotropic time ensures that once yielded these systems maintain a fluidized state, which prevents rapid oscillations between the gel and fluidized states. The balance between rapid fluidization and slow gelation effectively eliminates the instabilities and erratic

behavior that could occur under weak gradients that promote potentially uncoordinated (random) initiation zones that undergo both rapid initiation and arresting of yielding. The long thixotropic time (seconds) is a result of two factors: (1) long relaxation times of the macromolecules (μs) and (2) a low probability of a successful bonding event due to end-group bonding (1:1,000,000).

The model developed in this manuscript is for aqueous gel networks that are unique from conventionally crosslinked hydrogels, which have permanent crosslinks as opposed to the flickering bonds associated with the natural proteoglycan macromolecules and the gel networks modeled here. Interestingly, Gemini hydrogel contacts have occasionally demonstrated speed-independent friction regimes. One early hypothesis offered for the dissipative stresses in Gemini hydrogel contacts was that the dissipation resulted from fluid shearing through a hydrodynamic penetration depth into the hydrogel surface [44–46]. Models proposed by Milner for hydrodynamic penetration depth [47] suggest that the penetration depth should be on the order of the mesh size and not dependent on the surface shear speed. The predicted result as a function of speed is thus monotonically dependent on sliding speed (i.e., $\tau \propto V^1 \cdot \xi^{-1}$). However, as proposed by Meier et al., if the hydrodynamic penetration depth increases linearly with sliding speed, then the shear rate and the resulting shear stress would be constant [11]. Intuitively, increasing sliding speeds and deformations of the surface chains may actually work in the obverse and actually reduce the mesh-size and the hydrodynamic penetration depth rather than increasing it, but to our knowledge accurate measurements of the hydrodynamic penetration depths have not been reported, and this remains an open research problem.

Collectively, this expanding fluidized zone model and these findings make some biological sense. The model reveals that the lubrication is sensitive to the macromolecular quality of the gel-spanning networks (τ_o) and the water content that controls the high shear-rate viscosity (η_∞) but does not require a particular shape of the concentration profile. The long thixotropic recovery time ensures the stability of fluidized zone under conditions of weak gradients. Finally, this combination of properties provides a resilient and robust model for speed-invariant lubrication in biological systems.

Acknowledgements This manuscript is dedicated to the memory of our friend and colleague, Prof. Anne Neville. A.A.P. gratefully acknowledges funding support from the NSF CAREER award (CMMI-CAREER-2048043). A.C.D. acknowledges funding support from the NSF CAREER award (CMMI-CAREER-1751945). W.G.S. acknowledges funding support from Alcon Laboratories.

Author contributions A.A.P., A.C.D., and W.G.S. wrote the main manuscript text, developed the model, and prepared figures. All authors reviewed the manuscript.

Funding National Science Foundation, CMMI-CAREER-2048043, CMMI-CAREER-1751945, Alcon Laboratories

Data availability Data sharing not applicable—the article describes entirely theoretical research.

Declarations

Conflict of interest The authors declare no conflict of interest.

References

1. Erdemir, A., Martin, J.-M. (eds.): Elsevier, Amsterdam The Netherlands (2007)
2. Skotheim, J.M., Mahadevan, L.: Soft lubrication. *Phys. Rev. Lett.* **92**, 245509 (2004). <https://doi.org/10.1103/PhysRevLett.92.245509>
3. Jin, Z.M., Dowson, D.: Elastohydrodynamic lubrication in biological systems. *Proc. Inst. Mech. Eng. Part J J. Eng. Tribol.* **219**, 367–380 (2005). <https://doi.org/10.1243/135065005X33982>
4. Gong, J., Osada, Y.: Gel friction: a model based on surface repulsion and adsorption. *J. Chem. Phys.* **109**, 8062–8068 (1998). <https://doi.org/10.1063/1.477453>
5. Gong, J.P., Kagata, G., Osada, Y.: Friction of gels. 4. friction on charged gels. *J. Phys. Chem. B.* **103**, 6007–6014 (1999). <https://doi.org/10.1021/jp990256v>
6. Suzuki, A., Ishii, R., Yamakami, Y., Nakano, K.: Surface friction of thermoresponsive poly(N-isopropylacrylamide) gels in water. *Colloid Polym. Sci.* **289**, 561–568 (2011). <https://doi.org/10.1007/s00396-011-2387-y>
7. Pitenis, A.A., Urueña, J.M., Schulze, K.D., Nixon, R.M., Dunn, A.C., Krick, B.A., Sawyer, W.G., Angelini, T.E.: Polymer fluctuation lubrication in hydrogel gemini interfaces. *Soft Matter* **10**, 8955–8962 (2014). <https://doi.org/10.1039/C4SM01728E>
8. Dunn, A.C., Sawyer, W.G., Angelini, T.E.: Gemini interfaces in aqueous lubrication with hydrogels. *Tribol. Lett.* **54**, 59–66 (2014). <https://doi.org/10.1007/s11249-014-0308-1>
9. Urueña, J.M., Pitenis, A.A., Nixon, R.M., Schulze, K.D., Angelini, T.E., Sawyer, W.G.: Mesh size control of polymer fluctuation lubrication in gemini hydrogels. *Biotribology*. **1–2**, 24–29 (2015). <https://doi.org/10.1016/j.biotri.2015.03.001>
10. Pitenis, A.A., Urueña, J.M., Cooper, A.C., Angelini, T.E., Sawyer, W.G.: Superlubricity in gemini hydrogels. *J. Tribol.* (2016). <https://doi.org/10.1115/1.4032890>
11. Meier, Y.A., Zhang, K., Spencer, N.D., Simic, R.: Linking friction and surface properties of hydrogels molded against materials of different surface energies. *Langmuir* **35**, 15805–15812 (2019). <https://doi.org/10.1021/acs.langmuir.9b01636>
12. Simič, R., Spencer, N.D.: Controlling the friction of gels by regulating interfacial oxygen during polymerization. *Tribol. Lett.* **69**, 86 (2021). <https://doi.org/10.1007/s11249-021-01459-1>
13. Schurz, J., Ribitsch, V.: Rheology of synovial fluid. *Biorheology* **24**, 385–399 (1987). <https://doi.org/10.3233/BIR-1987-24404>
14. Bonnevie, E.D., Galesso, D., Secchieri, C., Cohen, I., Bonassar, L.J.: Elastoviscous transitions of articular cartilage reveal a

- mechanism of synergy between lubricin and hyaluronic acid. *PLoS ONE* **10**, e0143415 (2015). <https://doi.org/10.1371/journal.pone.0143415>
15. Martin-Alarcon, L., Schmidt, T.A.: Rheological effects of macromolecular interactions in synovial fluid. *Biorheology* **53**, 49–67 (2016). <https://doi.org/10.3233/BIR-15104>
 16. Klein, J.: Molecular mechanisms of synovial joint lubrication. *Proc. Inst. Mech. Eng. J. Eng. Tribol.* **220**, 691–710 (2006). <https://doi.org/10.1243/13506501JET143>
 17. Moore, A.C., Burris, D.L.: Tribological rehydration of cartilage and its potential role in preserving joint health. *Osteoarthr. Cartil.* **25**, 99–107 (2017). <https://doi.org/10.1016/j.joca.2016.09.018>
 18. Porte, E., Cann, P., Masen, M.: Fluid load support does not explain tribological performance of PVA hydrogels. *J. Mech. Behav. Biomed. Mater.* **90**, 284–294 (2019). <https://doi.org/10.1016/j.jmbbm.2018.09.048>
 19. de Beer, S., Kenmoé, G.D., Müser, M.H.: On the friction and adhesion hysteresis between polymer brushes attached to curved surfaces: rate and solvation effects. *Friction*, **3**, 148–160 (2015). <https://doi.org/10.1007/s40544-015-0078-2>
 20. Müser, M.H., Nicola, L.: Modeling the surface topography dependence of friction, adhesion, and contact compliance. *MRS Bull.* **47**, 1221–1228 (2022). <https://doi.org/10.1557/s43577-022-00468-2>
 21. Rudge, R.E.D., Scholten, E., Dijkman, J.A.: Natural and induced surface roughness determine frictional regimes in hydrogel pairs. *Tribol. Int.* **141**, 105903 (2020). <https://doi.org/10.1016/j.triboint.2019.105903>
 22. Charnley, J.: The lubrication of animal joints in relation to surgical reconstruction by arthroplasty. *Ann. Rheum. Dis.* **19**, 10–19 (1960). <https://doi.org/10.1136/ard.19.1.10>
 23. McCutchen, C.W.: The frictional properties of animal joints. *Wear* **5**, 1–17 (1962). [https://doi.org/10.1016/0043-1648\(62\)90176-X](https://doi.org/10.1016/0043-1648(62)90176-X)
 24. Dowson, D., Wright, V., Longfield, M.D.: Human joint lubrication. *Biomed. Eng. (NY)* **4**, 160–165 (1969)
 25. Lieleg, O., Vladescu, I., Ribbeck, K.: Characterization of particle translocation through mucin hydrogels. *Biophys. J.* **98**, 1782–1789 (2010). <https://doi.org/10.1016/j.bpj.2010.01.012>
 26. Pitenis, A.A., Urueña, J.M., Hart, S.M., O'Bryan, C.S., Marshall, S.L., Levings, P.P., Angelini, T.E., Sawyer, W.G.: Friction-induced inflammation. *Tribol. Lett.* **66**, 81 (2018). <https://doi.org/10.1007/s11249-018-1029-7>
 27. Meldrum, O.W., Yakubov, G.E., Bonilla, M.R., Deshmukh, O., McGuckin, M.A., Gidley, M.J.: Mucin gel assembly is controlled by a collective action of non-mucin proteins, disulfide bridges, Ca²⁺-mediated links, and hydrogen bonding. *Sci. Rep.* **8**, 1–16 (2018). <https://doi.org/10.1038/s41598-018-24223-3>
 28. Taylor, C., Draget, K.I., Pearson, J.P., Smidsrød, O.: Mucous systems show a novel mechanical response to applied deformation. *Biomacromol* **6**, 1524–1530 (2005). <https://doi.org/10.1021/bm049225i>
 29. Broughton-Head, V.J., Shur, J., Carroll, M.P., Smith, J.R., Shute, J.K.: Unfractionated heparin reduces the elasticity of sputum from patients with cystic fibrosis. *Am. J. Physiol. Cell. Mol. Physiol.* **293**, L1240–L1249 (2007). <https://doi.org/10.1152/ajplung.00206.2007>
 30. De Gennes, P.-G.: *Scaling Concepts in Polymer Physics*. Cornell University Press, New York (1979)
 31. Pitenis, A.A., Urueña, J.M., Nixon, R.M., Bhattacharjee, T., Krick, B.A., Dunn, A.C., Angelini, T.E., Sawyer, W.G.: Lubricity from entangled polymer networks on hydrogels. *J. Tribol.* (2016). <https://doi.org/10.1115/1.4032889>
 32. Mate, C.M., Carpick, R.W.: *Tribology on the small scale: a modern textbook on friction, lubrication, and wear*. Oxford University Press, Oxford (2019)
 33. Berman, A.D., Ducker, W.A., Israelachvili, J.N.: Origin and characterization of different stick–slip friction mechanisms. *Langmuir* **12**, 4559–4563 (1996). <https://doi.org/10.1021/la950896z>
 34. Jarrett, C.A., Ranawat, A.S., Bruzzone, M., Blum, Y.C., Rodriguez, J.A., Ranawat, C.S.: The squeaking hip: a phenomenon of ceramic-on-ceramic total hip arthroplasty. *J. Bone Jt. Surgery-American* **91**, 1344–1349 (2009). <https://doi.org/10.2106/JBJS.F.00970>
 35. Akay, A.: Acoustics of friction. *J. Acoust. Soc. Am.* **111**, 1525–1548 (2002). <https://doi.org/10.1121/1.1456514>
 36. Jin, Z., Dowson, D.: Bio-friction. *Friction* **1**, 100–113 (2013). <https://doi.org/10.1007/s40544-013-0004-4>
 37. Sridhar, M.: Anatomy of cornea and ocular surface. *Indian J. Ophthalmol.* **66**, 190 (2018). https://doi.org/10.4103/ijo.IJO_646_17
 38. Dunn, A.C., Tichy, J.A., Urueña, J.M., Sawyer, W.G.: Lubrication regimes in contact lens wear during a blink. *Tribol. Int.* **63**, 45–50 (2013). <https://doi.org/10.1016/j.triboint.2013.01.008>
 39. Tiffany, J.M.: The viscosity of human tears. *Int. Ophthalmol.* **15**, 371–376 (1991). <https://doi.org/10.1007/BF00137947>
 40. Gouveia, S.M., Tiffany, J.M.: Human tear viscosity: an interactive role for proteins and lipids. *Biochim. Biophys. Acta - Proteins Proteomics.* **1753**, 155–163 (2005). <https://doi.org/10.1016/j.bbapap.2005.08.023>
 41. Pitenis, A.A., Urueña, J.M., Hormel, T.T., Bhattacharjee, T., Niemi, S.R., Marshall, S.L., Hart, S.M., Schulze, K.D., Angelini, T.E., Sawyer, W.G.: Corneal cell friction: Survival, lubricity, tear films, and mucin production over extended duration in vitro studies. *Biotribology.* **11**, 77–83 (2017). <https://doi.org/10.1016/j.biotri.2017.04.003>
 42. Pedro, D.I., Nguyen, D.T., Rosa, J.G., Diodati, N., Kim, J., Bowman, J.I., Olson, R.A., Urueña, J.M., Sumerlin, B.S., Sawyer, W.G.: Gel-forming mucin improves lubricity across model gemini epithelial cell interfaces. *Tribol. Lett.* **69**, 155 (2021). <https://doi.org/10.1007/s11249-021-01529-4>
 43. Guvendiren, M., Lu, H.D., Burdick, J.A.: Shear-thinning hydrogels for biomedical applications. *Soft Matter* **8**, 260–272 (2012). <https://doi.org/10.1039/C1SM06513K>
 44. Duval, J.F.L., Zimmermann, R., Cordeiro, A.L., Rein, N., Werner, C.: Electrokinetics of diffuse soft interfaces. IV. Analysis of streaming current measurements at thermoresponsive thin films. *Langmuir* **25**, 10691–10703 (2009). <https://doi.org/10.1021/la9011907>
 45. Urueña, J.M., McGhee, E.O., Angelini, T.E., Dowson, D., Sawyer, W.G., Pitenis, A.A.: Normal load scaling of friction in gemini hydrogels. *Biotribology.* **13**, 30–35 (2018). <https://doi.org/10.1016/j.biotri.2018.01.002>
 46. McGhee, E.O., Urueña, J.M., Pitenis, A.A., Sawyer, W.G.: Temperature-dependent friction of gemini hydrogels. *Tribol. Lett.* **67**, 117 (2019). <https://doi.org/10.1007/s11249-019-1229-9>
 47. Milner, S.T.: Hydrodynamic penetration into parabolic brushes. *Macromolecules* **24**, 3704–3705 (1991). <https://doi.org/10.1021/ma00012a036>

Publisher's Note Springer Nature remains neutral with regard to jurisdictional claims in published maps and institutional affiliations.

Springer Nature or its licensor (e.g. a society or other partner) holds exclusive rights to this article under a publishing agreement with the author(s) or other rightsholder(s); author self-archiving of the accepted manuscript version of this article is solely governed by the terms of such publishing agreement and applicable law.